COMPUTER RESEARCH AND MODELING
2026 VOL. 18 NO. 2 P. 463–481
DOI: 10.20537/2076-7633-2026-18-2-463-481

Ки&М

ANALYSIS AND MODELING OF COMPLEX LIVING SYSTEMS

UDC: 519.8

A stage-structured delay model for biological control of Rugose Spiraling Whitefly in coconut plantations

E. Jenitta, R. Senthamarai[a]

Department of Mathematics, College of Engineering and Technology, SRM Institute of Science and Technology, Kattankulathur, 603 203, Tamil Nadu, India

E-mail: [a] senthamr@srmist.edu.in

Received 20.12.2025, after completion — 02.02.2026.
Accepted for publication 11.02.2026.

Coconut plantation plays a vital role in the economy and source of living for millions of farmers around the world, especially in tropical regions. The rugose spiraling whitefly is a highly destructive pest causing severe damage to coconut trees and significantly reducing their productivity. The aim of this paper is to develop and analyze a mathematical model that captures the dynamics of whitefly and to highlight the benefits of using biological control to mitigate the impact of pest damaging coconut palms. To be more realistic, a stage-structured model with maturation delay and lag in the implementation of the control measures has been considered in the model. We identify the equilibrium points of the system and perform a stability analysis to assess the system behavior. The numerical simulation of the proposed system is also reported. The findings reveal that introducing the population of parasitoids can effectively reduce the rugose spiraling whitefly population presenting a promising strategy for mitigating the pest's impact.

Keywords: pest control, Rugose Spiraling Whitefly, maturation delay, stability, Encarsia guadeloupae

Citation: *Computer Research and Modeling*, 2026, vol. 18, no. 2, pp. 463–481.

The authors are pleased to acknowledge the financial support of the Selective Excellence Research Initiative (SRMIST/R/AR(A)/SERI2023/174/31).

1. Introduction

Every species in the real world has a life cycle that is stage-structured, usually consisting of distinct immature and mature phases with varying biological processes, risk, and sustainable interactions. Stage-structured population models offer a more realistic framework for examining species dynamics than unstructured models and were developed as a result of this essential feature. Stage-structured models have become especially useful in the context of pest management. Numerous pest species experience developmental transitions or transformations that impact their rates of growth, the susceptibility to predators, and capacity to produce offspring. The impact of a distinct development delay in a single-species population model that includes immature and mature stages was investigated by Aiello and Freedman [Aiello, Freedman, 1990]. Their research showed how rich dynamical behavior, such as shifts in equilibrium stability and the emergence of oscillations, can result from even a small maturation delay. Since then, ecological systems have made extensive use of stage-structured models, particularly in the context of pest management. Designing successful control interventions requires accurately capturing these transitions. To better understand population behavior under diverse ecological conditions, many researchers have created and examined stage-structured models with and without delays [Bandyopadhyay, Banerjee, 2006; Banerjee et al., 2010; Jatav et al., 2014; Singh et al., 2016; Kumar et al., 2019; Suganya et al., 2024]. Biological realism in pest modeling is essential not only for theoretical accuracy but also for practical implementation in the field. For instance, while adults are mainly in charge of reproduction and spread, juvenile stages are frequently more susceptible to external influences or natural enemies. Decisions regarding the timing and kind of interventions, such as the use of pesticides, habitat management, or biological control, can be influenced by knowledge of how pest populations move through these phases. This emphasizes how stage-structured modeling is becoming more and more important in the context of integrated pest management, which uses a mix of biological, cultural, mechanical, and informational techniques to promote sustainable agriculture and lessen the dependence on chemical pesticides [Zhou et al., 2024].

Biological control agents, especially parasitoids, have been successfully used to combat a range of agricultural pests and are an essential part of integrated pest management [Dhaliwal, Arora, 1996]. In contrast to predators, parasitoids frequently target particular stages of the pest's growth and ultimately kill its host in order to finish their entire life cycle. They are excellent options for incorporation in stage-structured models because of their unique characteristics. If the time frame and amount of release are carefully considered, the introduction of parasitoids can dramatically lower the number of pests while maintaining the sustainability of the environment [DeBach, Rosen, 1991]. Awareness-based interventions are receiving more attention as a supplemental control measure to biological control. These encompass teaching farmers and other interested parties about pest identification, monitoring, control techniques, and the advantages of environmentally friendly practices [Khan et al., 2013]. Various mathematical models have been proposed by researchers to study the impact of awareness-based measures in pest management and adulteration control [Al Basir et al., 2018; Al Basir et al., 2019; Al Basir, 2020; Abraha et al., 2021; Mathur et al., 2021].

The motivation for this study arises from the increasing threat posed by the Rugose Spiraling Whitefly (RSW) (*Aleurodicus rugioperculatus*) to coconut plantations, particularly in tropical and subtropical regions. First reported in India in 2016, RSW has become a significant pest, severely affecting coconut trees by feeding on plant sap and producing copious honeydew, which fosters the growth of sooty mold and disrupts photosynthesis [Selvaraj et al., 2017]. According to field-based surveys and entomological studies, the life cycle of RSW comprises distinct stages — eggs, multiple nymphal instars, pupae, and adults — each with specific biological roles and vulnerabilities. For instance, the nymphs and adults feed on plant sap, while the eggs and pupae are largely sessile but contribute to rapid population growth under favorable conditions [Saranya et al., 2021]. This well-defined stage structure makes RSW an ideal candidate for stage-structured modeling approaches,

particularly when designing targeted pest control strategies. Because of its protective waxy spirals and high fecundity, the pest is especially challenging to manage with traditional pesticides [Elango, Nelson, 2020]. As a result, farmer awareness campaigns in conjunction with biological control employing parasitoids like *Encarsia guadeloupae* have become a viable and ecologically conscious strategy [Rao et al., 2018; Selvaraj et al., 2020; Suriya et al., 2021]. Parameter values have been chosen based on biological and field data unique to the RSW coconut system in order to guarantee the model's practical relevance. A key novelty of this work is the incorporation of two realistic time delays governing the dynamics of rugose spiraling whitefly and coconut palms. The maturation delay captures the time required for RSW to develop into reproductive adults, influencing population growth and oscillatory behavior. The awareness delay represents the lag between the implementation of management awareness programs and their effective impact on coconut pest control. Mathematical models for the population dynamics of RSW in coconut trees have been proposed primarily using systems of ordinary differential equations (ODEs) [Govindaraj, Rathinam, 2022; Suganya, Senthamarai, 2022a; Suganya, Senthamarai, 2022b]. These models typically focus on pest growth, spread, and interactions with environmental factors or control agents. However, most of these models do not incorporate time delays. Delay differential equations (DDEs) provide a natural framework for modeling biological and ecological systems where time lags play a critical role in the dynamics [Hale, 1969; Huang, 1993; Santra et al., 2023; Dhivyadharshini, Senthamarai, 2024; Ismail et al., 2024]. This present study refines upon earlier work by introducing a delayed stage-structured model that better reflects the temporal complexities.

The structure of the paper is as follows. Section 2 presents a mathematical model of the system. Section 3 discusses positivity, boundedness, and equilibrium analysis, including the basic reproduction number. Section 4 provides a sensitivity analysis of the parameters. Section 5 presents numerical evidence of the analytical conditions obtained in the previous sections. Section 6 concludes the proposed system model.

2. Mathematical formulation of the problem

To derive the proposed model, we consider the population dynamics of rugose spiraling whitefly in coconut plantations under biological control and awareness-based interventions. Whitefly populations exhibit a well-defined stage structure consisting of immature stages (eggs and nymphs) and reproductive adults [Selvaraj et al., 2017; Saranya et al., 2021]. Accordingly, the pest population is divided into immature pests $X(t)$ and mature pests $Y(t)$, following standard stage-structured modeling approaches [Aiello, Freedman, 1990; Bandyopadhyay, Banerjee, 2006; Kumar et al., 2019].

We assume that mature whiteflies lay eggs at a per capita rate α, contributing to the recruitment of immature individuals. The immature pest population decreases due to parasitization by parasitoids at rate ϕ and experience natural mortality at rate d_1. Since individuals require a fixed maturation time τ_1 to become adults and experience mortality during this period, only a fraction $e^{-d_1\tau_1}$ survives to maturity [Aiello, Freedman, 1990; Bandyopadhyay, Banerjee, 2006]. Thus, the dynamics of the immature pest population are governed by

$$\frac{dX(t)}{dt} = \alpha Y(t) - \phi X(t)S(t) - \alpha e^{-d_1\tau_1} Y(t-\tau_1) - d_1 X(t). \tag{1}$$

The mature pest population increases through recruitment from the immature class after the maturation delay τ_1. It decreases due to natural mortality at rate d_2 and awareness-based management interventions at a rate γ. The effect of awareness is not instantaneous; hence, we assume that it becomes effective after a delay τ_2, representing the time lag between information dissemination and implementation of control actions. Hence, the dynamics of the mature pest population are described by

$$\frac{dY(t)}{dt} = \alpha e^{-d_1\tau_1} Y(t-\tau_1) - d_2 Y(t) - \gamma A(t-\tau_2)Y(t). \tag{2}$$

Biological control is incorporated through parasitoids, *Encarsia guadeloupae*, which preferentially attack early developmental stages of rugose spiraling whitefly and significantly reduce juvenile survival [Selvaraj et al., 2020; Suriya et al., 2021]. Successful parasitization contributes to parasitoid reproduction with conversion efficiency ϕ_1, while parasitoids experience natural mortality at rate d_3. Accordingly, the parasitoid population dynamics represented by $S(t)$ are given by

$$\frac{dS(t)}{dt} = \phi_1 \phi X(t) S(t) - d_3 S(t). \tag{3}$$

In practice, pest management is also influenced by farmers' awareness and response to infestation levels [Khan et al., 2013; Abraha et al., 2021; Zhou et al., 2024]. To capture this effect, an awareness variable $A(t)$ is introduced. We further assume that the level of awareness increases with mature pest density at rate h and through baseline awareness programs at rate r, while it decays naturally at rate η. The awareness dynamics are therefore modeled as

$$\frac{dA(t)}{dt} = r + hY(t) - \eta A(t). \tag{4}$$

With the above assumptions, the model for the dynamics of rugose spiraling whitefly, parasitoids, and the level of farmer awareness is given by

$$\begin{aligned}
\frac{dX(t)}{dt} &= \alpha Y(t) - \phi X(t) S(t) - \alpha e^{-d_1 \tau_1} Y(t - \tau_1) - d_1 X(t), \\
\frac{dY(t)}{dt} &= \alpha e^{-d_1 \tau_1} Y(t - \tau_1) - d_2 Y(t) - \gamma A(t - \tau_2) Y(t), \\
\frac{dS(t)}{dt} &= \phi_1 \phi X(t) S(t) - d_3 S(t), \\
\frac{dA(t)}{dt} &= r + hY(t) - \eta A(t),
\end{aligned} \tag{5}$$

with the initial conditions

$$X(\psi) > 0, \quad Y(\psi) > 0, \quad S(\psi) > 0, \quad A(\psi) > 0, \tag{6}$$

where $\psi \in [-\tau, 0]$ with $\tau = \max\{\tau_1, \tau_2\}$.

3. Model analysis

3.1. Positivity and boundedness

Theorem 1. *For positive initial data, solutions of system* (5) *are positive for all* $t \geqslant 0$.

Proof. From the third equation of (5),

$$\frac{dS}{dt} = \phi_1 \phi X S - d_3 S.$$

Integrating and using the initial condition, we obtain

$$S(t) = S(0) \exp\left(\int_0^t [\phi_1 \phi X(\chi) S(\chi) - d_3 S(\chi)] \, d\chi \right).$$

This implies $S(t) > 0$ for all $t > 0$ since $S(0) > 0$. Hence, $S(t)$ remains positive for all $t > 0$.

To establish positivity of $A(t)$, let $t_1 > 0$ be the first time such that $A(t_1) = 0$. From the last equation of (5), at $t = t_1$ we have

$$\frac{dA}{dt} = r + hY(t_1) - \eta A(t_1) > 0,$$

which implies $A(t) > 0$ for all $t > 0$. Using a similar argument, it can be shown that $X(t) > 0$ and $Y(t) > 0$ for all $t > 0$. Hence, a solution of the initial value problem (5)–(6) exists in the region $\mathbb{R}^4_+$ and remains nonnegative for all $t > 0$, following the fundamental lemma in [Yang et al., 1996].

Theorem 2. *All solutions of system* (5) *with nonnegative initial conditions are uniformly bounded for* $t \geqslant 0$.

Proof. Define the total pest population by

$$P(t) = X(t) + Y(t). \tag{7}$$

Adding the first two equations of system (5), we obtain

$$\frac{dP(t)}{dt} = \alpha Y(t) - d_1 X(t) - d_2 Y(t) - \phi X(t) S(t) - \gamma A(t - \tau_2) Y(t). \tag{8}$$

Since all state variables are nonnegative,

$$\frac{dP(t)}{dt} \leqslant \alpha Y(t) - d_1 X(t) - d_2 Y(t). \tag{9}$$

Let $d = \min\{d_1, d_2\}$. Then

$$\frac{dP(t)}{dt} \leqslant (\alpha - d) P(t). \tag{10}$$

Therefore,

$$P(t) \leqslant P(0) e^{(\alpha - d)t}. \tag{11}$$

Hence, there exists a constant

$$M_1 = \sup_{s \in [-\tau, 0]} (X(s) + Y(s)) e^{(\alpha - d)\tau} \tag{12}$$

such that

$$X(t) + Y(t) \leqslant M_1, \quad t \geqslant 0. \tag{13}$$

From the fourth equation of system (5),

$$\frac{dA(t)}{dt} = r + hY(t) - \eta A(t) \leqslant r + hM_1 - \eta A(t). \tag{14}$$

Therefore,

$$A(t) \leqslant M_2 := \max\left\{A(0), \frac{r + hM_1}{\eta}\right\}, \quad t \geqslant 0. \tag{15}$$

Similarly, from the third equation of system (5),

$$\frac{dS(t)}{dt} = S(t)(\phi_1 \phi X(t) - d_3) \leqslant S(t)(\phi_1 \phi M_1 - d_3). \tag{16}$$

Hence,

$$S(t) \leqslant M_3 := \begin{cases} S(0), & \text{if } \phi_1 \phi M_1 \leqslant d_3, \\ S(0) e^{(\phi_1 \phi M_1 - d_3)\tau}, & \text{otherwise.} \end{cases} \tag{17}$$

Further, letting

$$M = \max\{M_1, M_2, M_3\}, \tag{18}$$

we obtain

$$0 \leqslant X(t), Y(t), S(t), A(t) \leqslant M, \quad t \geqslant 0. \tag{19}$$

Thus, all solutions of system (5) are uniformly bounded in $\mathbb{R}^4_+$.

3.2. Basic reproduction number

The system's basic reproduction number is provided by $R_0 = \frac{\eta\alpha e^{-d_1\tau_1}}{\gamma r+\eta d_2}$.

The next-generation matrix method is used to obtain the expression for the basic reproduction number [Heffernan et al., 2005]. Let $Z = (X, Y)^T$.

We write

$$Z' = F(Z) - V(Z), \tag{20}$$

where

$$F(Z) = \begin{bmatrix} \alpha Y \\ \alpha e^{-d_1\tau_1} Y \end{bmatrix} \quad \text{and} \quad V(Z) = \begin{bmatrix} -\phi XS - \alpha e^{-d_1\tau_1} Y - d_1 X \\ -d_2 Y - \gamma AY \end{bmatrix}. \tag{21}$$

The Jacobian matrix of $F(Z)$ and $V(Z)$ denoted by $DF(E_1)$ and $DV(E_1)$, at the pest-free equilibrium point E_1 respectively, are given as follows:

$$DF(E_1) = \begin{bmatrix} 0 & \alpha \\ 0 & \alpha e^{-d_1\tau_1} \end{bmatrix} \quad \text{and} \quad DV(E_1) = \begin{bmatrix} -d_1 & -\alpha e^{-d_1\tau_1} \\ 0 & -d_2 - \frac{\gamma r}{\eta} \end{bmatrix}. \tag{22}$$

The spectral radius of $DF(E_1)(DV(E_1))^{-1}$ gives the reproduction number. Thus,

$$R_0 = \frac{\eta\alpha e^{-d_1\tau_1}}{\gamma r + \eta d_2}.$$

3.3. Stability analysis of the system

Equilibrium points

We consider the following equilibrium points for the model (5):

(i) The pest-free equilibrium $E_1\left(0, 0, 0, \frac{r}{\eta}\right)$.

(ii) The co-existence equilibrium $E_2(X^*, Y^*, S^*, A^*)$ exists when **(H1)** is satisfied

where

$$X^* = \frac{d_3}{\phi\phi_1}, \quad Y^* = \frac{\eta\alpha e^{-d_1\tau_1} - \gamma r_0 - \eta d_2}{h\gamma}, \quad A^* = \frac{\alpha e^{-d_1\tau_1} - d_2}{\gamma},$$

$$S^* = \frac{-1}{\gamma h\phi d_3}\left[\left(e^{-d_1\tau_1}\right)^2 \alpha^2\eta\phi\phi_1 - e^{-d_1\tau_1}\gamma\alpha\phi\phi_1 r_0 - e^{-d_1\tau_1}\alpha^2\eta\phi\phi_1 - e^{-d_1\tau_1}\alpha\eta\phi\phi_1 d_2 + \right.$$
$$\left. + \gamma\alpha\phi\phi_1 r_0 + \alpha\eta\phi\phi_1 d_2 + d_1 d_3\gamma h\right]$$

and

$$(\mathbf{H1}): \qquad \tau_1 < \frac{1}{d_1}\ln\left(\frac{\eta\alpha}{\gamma r_0 + \eta d_2}\right) =: \tau_{10}. \tag{23}$$

The following is obtained by linearizing the system around the equilibrium point:

$$\frac{dL(t)}{dt} = FL(t) + GL(t-\tau_1) + HL(t-\tau_2), \tag{24}$$

where F, G and H are 4×4 matrices defined as follows:

$$F = [f_{ij}] = \begin{pmatrix} -\phi S^* - d_1 & \alpha & -\phi X^* & 0 \\ 0 & -d_2 - \gamma A^* & 0 & 0 \\ \phi_1 \phi S^* & 0 & \phi_1 \phi X^* - d_3 & 0 \\ 0 & h & 0 & -\eta \end{pmatrix}, \tag{25}$$

$$G = [g_{ij}] = \begin{pmatrix} 0 & -\alpha e^{-d_1 \tau_1} & 0 & 0 \\ 0 & \alpha e^{-d_1 \tau_1} & 0 & 0 \\ 0 & 0 & 0 & 0 \\ 0 & 0 & 0 & 0 \end{pmatrix}, \tag{26}$$

$$H = [h_{ij}] = \begin{pmatrix} 0 & 0 & 0 & 0 \\ 0 & 0 & 0 & -\gamma Y^* \\ 0 & 0 & 0 & 0 \\ 0 & 0 & 0 & 0 \end{pmatrix}. \tag{27}$$

The characteristic equation of the delay system (5) is given by

$$L(\lambda) = \left| \lambda I - F - e^{-\lambda \tau_1} G - e^{-\lambda \tau_2} H \right| = 0. \tag{28}$$

This gives

$$\lambda^4 + a_1 \lambda^3 + a_2 \lambda^2 + a_3 \lambda + a_4 + e^{-\lambda \tau_1} \left(b_1 \lambda^3 + b_2 \lambda^2 + b_3 \lambda + b_4 \right) + e^{-\lambda \tau_2} \left(c_1 \lambda^2 + c_2 \lambda + c_3 \right) = 0 \tag{29}$$

where,

$$\begin{aligned}
a_1 &= A^* \gamma - X^* \phi \phi_1 - f_{11} + d_2 + d_3 + \eta, \\
a_2 &= A^* \gamma d_3 - f_{11} A^* \gamma - A^* X^* \gamma \phi \phi_1 + S^* X^* \phi^2 \phi_1 + A^* \gamma \eta + \eta d_2 + \eta d_3 + d_2 d_3 - \\
&\quad - f_{11} \eta - f_{11} d_2 - f_{11} d_3 - X^* \eta \phi \phi_1 - X^* d_2 \phi \phi_1 + f_{11} X^* \phi \phi_1, \\
a_3 &= \eta d_2 d_3 - f_{11} \eta d_2 - f_{11} \eta d_3 - f_{11} d_2 d_3 + S^* X^* \eta \phi^2 \phi_1 - X^* \eta d_2 \phi \phi_1 + \\
&\quad + f_{11} X^* \eta \phi \phi_1 + f_{11} X^* d_2 \phi \phi_1 + S^* X^* d_2 \phi^2 \phi_1 + f_{11} A^* X^* \gamma \phi \phi_1 - A^* X^* \gamma \eta \phi \phi_1 + \\
&\quad + A^* S^* X^* \gamma \phi^2 \phi_1 + A^* \gamma \eta d_3 - f_{11} A^* \gamma \eta - f_{11} A^* \gamma d_3, \\
a_4 &= -f_{11} \eta d_2 d_3 + f_{11} X^* \eta d_2 \phi \phi_1 + S^* X^* \eta d_2 \phi^2 \phi_1 + f_{11} A^* X^* \gamma \eta \phi \phi_1 + \\
&\quad + A^* S^* X^* \gamma \eta \phi^2 \phi_1 - f_{11} A^* \gamma \eta d_3, \\
b_1 &= -\alpha e^{-d_1 \tau_1}, \\
b_2 &= \alpha e^{-d_1 \tau_1} X^* \phi \phi_1 - \alpha e^{-d_1 \tau_1} \eta + f_{11} \alpha e^{-d_1 \tau_1} - \alpha e^{-d_1 \tau_1} d_3, \\
b_3 &= -\alpha e^{-d_1 \tau_1} S^* X^* \phi^2 \phi_1 - \alpha e^{-d_1 \tau_1} X^* \eta \phi \phi_1 + f_{11} \alpha e^{-d_1 \tau_1} X^* \phi \phi_1 - f_{11} \alpha e^{-d_1 \tau_1} \eta + \\
&\quad + \alpha e^{-d_1 \tau_1} \eta d_3 - f_{11} \alpha e^{-d_1 \tau_1} d_3, \\
b_4 &= -\left(\alpha e^{-d_1 \tau_1} S^* X^* \eta \phi^2 \phi_1 + f_{11} \alpha e^{-d_1 \tau_1} X^* \eta \phi \phi_1 - f_{11} \alpha e^{-\mu_I \tau_1} \eta d_3 \right), \\
c_1 &= Y^* \gamma h, \\
c_2 &= -\left(X^* Y^* \gamma h \phi \phi_1 + f_{11} Y^* \gamma h - Y^* \gamma h d_3 \right), \\
c_3 &= S^* X^* Y^* \gamma h \phi^2 \phi_1 + f_{11} X^* Y^* \gamma h \phi \phi_1 - f_{11} Y^* \gamma h d_3.
\end{aligned}$$

The stability requirements for the equilibrium E_2 are discussed below.

Case I: When $\tau_1 = 0$ and $\tau_2 = 0$

The characteristic equation reduces to

$$\lambda^4 + \mathcal{A}_1\lambda^3 + \mathcal{A}_2\lambda^2 + \mathcal{A}_3\lambda + \mathcal{A}_4 = 0 \tag{30}$$

where $\mathcal{A}_1 = a_1 + b_1$, $\mathcal{A}_2 = a_2 + b_2 + c_1$, $\mathcal{A}_3 = a_3 + b_3 + c_2$, $\mathcal{A}_4 = a_4 + b_4 + c_3$.

The roots of the characteristic equation will have negative real parts when $\mathcal{A}_1 > 0$, $\mathcal{A}_4 > 0$, $\mathcal{A}_1\mathcal{A}_2 - \mathcal{A}_3 > 0$ and $\mathcal{A}_1\mathcal{A}_2\mathcal{A}_3 - \mathcal{A}_3^2 - \mathcal{A}_4\mathcal{A}_1^2 > 0$. Hence, the system (5) around E_2 is LAS.

Case II: When $\tau_1 > 0$ and $\tau_2 = 0$

Equation (29) becomes

$$\lambda^4 + A_1\lambda^3 + A_2\lambda^2 + A_3\lambda + A_4 + e^{-\lambda\tau_1}\left(b_1\lambda^3 + b_2\lambda^2 + b_3\lambda + b_4\right) = 0, \tag{31}$$

where $A_1 = a_1$, $A_2 = a_2 + c_1$, $A_3 = a_3 + c_2$, $A_4 = a_4 + c_3$. Now, equation (31) can be written as

$$P(\lambda, \tau_1) + Q(\lambda, \tau_1)e^{-\lambda\tau_1} = 0, \tag{32}$$

where $P = \lambda^4 + A_1\lambda^3 + A_2\lambda^2 + A_3\lambda + A_4$ and $Q = b_1\lambda^3 + b_2\lambda^2 + b_3\lambda + b_4$.

As above, due to the dependence of the coefficients of the polynomials $P(\lambda, \tau_1)$ and $Q(\lambda, \tau_1)$ on τ_1, we apply the geometric criterion of stability switch [An et al., 2019]. For this, the following conditions should be satisfied.

(i) Equation (32) has no zero root, that is, $A_4 + b_4 \neq 0$, i. e., $A_4 + B_4 + C_4 + D_4 \neq 0$.

(ii) For $\lambda = i\kappa$, $\kappa \in \mathbb{R}$, $P(i\kappa, \tau_1) + Q(i\kappa, \tau_1) \neq 0$, $\tau_1 \in \mathbb{R}$, i. e., $\kappa^4 - (A_2 + b_2)\kappa^2 + (A_4 + b_4) - i\left\{(A_1 + b_1)\kappa^3 - (A_3 + b_3)\kappa\right\} \neq 0$.

(iii)

$$\lim_{|\rho|\to\infty}\left|\frac{Q(\rho, \tau_1)}{P(\rho, \tau_1)}\right| < 1$$

when $\mathrm{Re}(\lambda) \geqslant 0$ for any τ_1.

(iv) $F(\kappa, \tau_1) = |P(i\kappa, \tau_1)|^2 - |Q(i\kappa, \tau_1)|^2$ for each τ_1 has at most a finite number of real zeros which is obvious as $F(\kappa, \tau_1)$ is a polynomial of degree eight.

(v) Each positive root $\kappa(\tau_1)$ of $F(\kappa, \tau_1) = 0$ is continuous and differentiable in τ_1 whenever it exists. Using the implicit function theorem, we can show that this condition holds. Let $\lambda = \zeta + i\kappa$, then equation (32) becomes

$$\begin{aligned}\zeta^4 + i4\zeta^3\kappa - 6\zeta^2\kappa^2 - i4\zeta\kappa^3 + \kappa^4 + A_1\left(\zeta^3 + i3\zeta^2\kappa - 3\zeta\kappa^2 - i\kappa^3\right) + \\ + A_2\left(\zeta^2 - \kappa^2 + i2\zeta\kappa\right) + A_3(\zeta + i\kappa) + A_4 + \Big[b_1\left(\zeta^3 + i3\zeta^2\kappa - 3\zeta\kappa^2 - i\kappa^3\right) + \\ + b_2\left(\zeta^2 - \kappa^2 + i2\zeta\kappa\right) + b_3(\zeta + i\kappa) + b_4\Big]e^{-\zeta\tau_1}(\cos\kappa\tau_1 - i\sin\kappa\tau_1) = 0.\end{aligned} \tag{33}$$

Comparing real and imaginary parts, we have

$$\begin{aligned}\zeta^4 + \kappa^4 - 6\zeta^2\kappa^2 + A_1\left(\zeta^3 - 3\zeta\kappa^2\right) + A_2\left(\zeta^2 - \kappa^2\right) + A_3\zeta + A_4 + \Big[b_1\left(\zeta^3 - 3\zeta\kappa^2\right) + \\ + b_2\left(\zeta^2 - \kappa^2\right) + b_3\zeta + b_4\Big]e^{-\zeta\tau_1}\cos\kappa\tau_1 + \left[b_1\left(3\zeta^2\kappa - \kappa^3\right) + 2b_2\zeta\kappa + b_3\kappa\right] - e^{-\zeta\tau_1}\sin\kappa\tau_1 = 0\end{aligned} \tag{34}$$

and

$$\begin{aligned}4\zeta^3\kappa - 4\zeta\kappa^3 + A_1\left(3\zeta^2\kappa - \kappa^3\right) + 2A_2\zeta\kappa + A_3\kappa + \left[b_1\left(3\zeta^2\kappa - \kappa^3\right) + 2b_2\zeta\kappa + b_3\kappa\right]\times \\ \times e^{-\zeta\tau_1}\cos\kappa\tau_1 - \left[b_1\left(\zeta^3 - 3\zeta\kappa^2\right) + b_2\left(\zeta^2 - \kappa^2\right) + b_3\zeta + b_4\right]e^{-\zeta\tau_1}\sin\kappa\tau_1 = 0.\end{aligned} \tag{35}$$

For a purely imaginary root $\zeta = 0$, so from (34) and (35):

$$\left(b_4 - b_2\kappa^2\right)\cos\kappa\tau_1 + \left(b_3\kappa - b_1\kappa^3\right)\sin\kappa\tau_1 = -\left(\kappa^4 - A_2\kappa^2 + A_4\right), \tag{36}$$

$$\left(b_3\kappa - b_1\kappa^3\right)\cos\kappa\tau_1 - \left(b_4 - b_2\kappa^2\right)\sin\kappa\tau_1 = A_1\kappa^3 - A_3\kappa. \tag{37}$$

Solving equations (36) and (37), we have

$$\sin\kappa\tau_1 = \frac{-\left(\kappa^4 - A_2\kappa^2 + A_4\right)\left(b_3\kappa - b_1\kappa^3\right) - \left(b_4 - b_2\kappa^2\right)\left(A_1\kappa^3 - A_3\kappa\right)}{\left(b_3\kappa - b_1\kappa^3\right)^2 + \left(b_4 - b_2\kappa^2\right)^2}, \tag{38}$$

$$\cos\kappa\tau_1 = \frac{\left(b_3\kappa - b_1\kappa^3\right)\left(A_1\kappa^3 - A_3\kappa\right) - \left(b_4 - b_2\kappa^2\right)\left(\kappa^4 - A_2\kappa^2 + A_4\right)}{\left(b_3\kappa - b_1\kappa^3\right)^2 + \left(b_4 - b_2\kappa^2\right)^2}. \tag{39}$$

Squaring and adding equations (36) and (37), we have

$$F(\kappa, \tau_1) = \kappa^8 + \left(A_1^2 - 2A_2 - b_1^2\right)\kappa^6 + \left(A_2^2 + 2A_4 - 2A_1A_3 + 2b_1b_3 - b_2^2\right)\kappa^4 + \\ + A_3^2 - 2A_2A_4 + 2b_2b_4 - b_3^2\kappa^2 + A_4^2 - b_4^2 = 0. \tag{40}$$

Let us assume $\tau_1 \in I_1 \subseteq \mathbb{R}_{+0}$ is the set where $\kappa(\tau_1)$ is a positive root of the above equation (40) and for $\tau_1 \notin I_1$, $\kappa(\tau_1)$ is not definite. Now define $\phi(\tau_1) \in [0, 2\pi)$ such that $\sin\phi(\tau_1)$ and $\cos\phi(\tau_1)$ is given by the right-hand side of equations (38) and (39).

Now for each $n \in N_0$, define a map $\tau_{1n}^{(1)}: I_1 \to \mathbb{R}_{+0}$, and stability switch occurs for the τ_1 values at which

$$\tau_{1n}^{(1)}(\tau_1) = \tau_1 \quad \text{for some } n$$

where

$$\tau_{1n}^{(1)} = \frac{\phi(\tau_1) + 2n\pi}{\kappa(\tau_1)}$$

for $n \in N_0$. That is, the stability switch takes place at the zeros of the functions

$$S_n^{(2)}(\tau_1) = \tau_1 - \tau_{1n}^{(1)}(\tau_1) \quad \text{for some } n \in N_0.$$

Now differentiating (34) and (35) with respect to τ_1, we get

$$\varphi_1\frac{d\zeta}{d\tau_1} + \varphi_2\frac{d\kappa}{d\tau_1} + \varphi_3 = 0, \tag{41}$$

$$-\varphi_2\frac{d\zeta}{d\tau_1} + \varphi_1\frac{d\kappa}{d\tau_1} + \varphi_4 = 0, \tag{42}$$

where

$$\varphi_1 = 4\zeta^3 - 12\zeta\kappa^2 + 3A_1\left(\zeta^2 - \kappa^2\right) + 2A_2\zeta + A_3 + \left[3b_1\left(\zeta^2 - \kappa^2\right) + 2b_2\zeta + \right. \\ \left. + b_3 - \tau_1b_1\left(\zeta^3 - 3\zeta\kappa^2\right) + b_2\left(\zeta^2 - \kappa^2\right) + b_3\zeta + b_4\right]e^{-\zeta\tau_1}\cos\kappa\tau_1 + \\ + \left[2\kappa(3b_1\zeta + b_2) - \tau_1b_1\left(3\zeta^2\kappa - \kappa^3\right) + 2b_2\zeta\kappa + b_3\kappa\right]e^{-\zeta\tau_1}\sin\kappa\tau_1,$$

$$\varphi_2 = 4\kappa^4 - 12\zeta^2\kappa - 6A_1\zeta\kappa - 2A_2\kappa - \left[2\kappa(3b_1\zeta + b_2) - \tau_1b_1\left(3\zeta^2\kappa - \kappa^3\right) + \right. \\ \left. + 2b_2\zeta\kappa + b_3\kappa\right]e^{-\zeta\tau_1}\cos\kappa\tau_1 + 3b_1\left(\zeta^2 - \kappa^2\right) + 2b_2\zeta + b_3 - \\ - \tau_1b_1\left(\zeta^3 - 3\zeta\kappa^2\right) + b_2\left(\zeta^2 - \kappa^2\right) + b_3\zeta + b_4e^{-\zeta\tau_1}\sin\kappa\tau_1,$$

$$\varphi_3 = \left[\frac{db_1}{d\tau_1}\left(\zeta^3 - 3\zeta\kappa^2\right) + \frac{db_2}{d\tau_1}\left(\zeta^2 - \kappa^2\right) + \frac{db_3}{d\tau_1}\zeta + \frac{db_4}{d\tau_1}\right] e^{-\zeta\tau_1}\cos\kappa\tau_1 -$$
$$- \left[b_1\left(\zeta^3 - 3\zeta\kappa^2\right) + b_2\left(\zeta^2 - \kappa^2\right) + b_3\zeta + b_4\right](\zeta\cos\kappa\tau_1 + \kappa\sin\kappa\tau_1)e^{-\zeta\tau_1} +$$
$$+ \left[\frac{db_1}{d\tau_1}\left(3\zeta^2\kappa - \kappa^3\right) + 2\frac{db_2}{d\tau_1}\zeta\kappa + \frac{db_3}{d\tau_1}\kappa\right] e^{-\zeta\tau_1}\sin\kappa\tau_1 +$$
$$+ \left[b_1\left(3\zeta^2\kappa - \kappa^3\right) + 2b_2\zeta\kappa + b_3\kappa\right](\kappa\cos\kappa\tau_1 - \zeta\sin\kappa\tau_1)e^{-\zeta\tau_1},$$

$$\varphi_4 = \left[\frac{db_1}{d\tau_1}\left(3\zeta^2\kappa - \kappa^3\right) + 2\frac{db_2}{d\tau_1}\zeta\kappa + \frac{db_3}{d\tau_1}\kappa\right] e^{-\zeta\tau_1}\cos\kappa\tau_1 -$$
$$- \left[b_1\left(3\zeta^2\kappa - \kappa^3\right) + 2b_2\zeta\kappa + b_3\kappa\right](\zeta\cos\kappa\tau_1 + \kappa\sin\kappa\tau_1)e^{-\zeta\tau_1} -$$
$$- \left[\frac{db_1}{d\tau_1}\left(\zeta^3 - 3\zeta\kappa^2\right) + \frac{db_2}{d\tau_1}\left(\zeta^2 - \kappa^2\right) + \frac{db_3}{d\tau_1}\zeta + \frac{db_4}{d\tau_1}\right] e^{-\zeta\tau_1}\sin\kappa\tau_1 +$$
$$+ \left[b_1\left(\zeta^3 - 3\zeta\kappa^2\right) + b_2\left(\zeta^2 - \kappa^2\right) + b_3\zeta + b_4\right](\zeta\sin\kappa\tau_1 - \kappa\cos\kappa\tau_1)e^{-\zeta\tau_1}.$$

Therefore, from equations (41) and (42), we get

$$\frac{d\zeta}{d\tau_1} = \frac{\varphi_2\varphi_4 - \varphi_1\varphi_3}{\varphi_1^2 + \varphi_2^2}.$$

Hence we have the following theorem:

Theorem 3. *Assume that* $\kappa(\tau_1)$ *is a positive real root of* (40)*, defined for* $\tau_1 \in I_1$*,* $I_1 \subseteq \mathbb{R}_{+0}$*, and at some* $\tau_1^* \in I_1$*,*

$$S_n^{(1)}\left(\tau_1^*\right) = 0 \quad \textit{for some } n \in N_0.$$

Then a pair of simple conjugate pure imaginary roots $\lambda_+\left(\tau_1^*\right) = i\kappa\left(\tau_1^*\right)$*,* $\lambda_-\left(\tau_1^*\right) = -i\kappa\left(\tau_1^*\right)$ *of* (34) *exists at* $\tau_1 = \tau_1^*$ *which crosses the imaginary axis from left to right if* $\Delta_1\left(\tau_1^*\right) > 0$ *and crosses the imaginary axis from right to left if* $\Delta_1\left(\tau_1^*\right) < 0$*, where*

$$\Delta_1\left(\tau_1^*\right) = \operatorname{sign}\left\{\frac{d\,\mathrm{Re}(\lambda)}{d\tau_1}\bigg|_{\lambda=i\kappa\left(\tau_1^*\right)}\right\} = \operatorname{sign}\left\{\frac{\varphi_2\varphi_4 - \varphi_3\varphi_1}{\varphi_1^2 + \varphi_2^2}\bigg|_{\lambda=i\kappa\left(\tau_1^*\right)}\right\}. \tag{43}$$

Case III: When $\tau_1 = 0$ **and** $\tau_2 > 0$

Equation (29) becomes

$$\lambda^4 + a_1\lambda^3 + a_2\lambda^2 + a_3\lambda + a_4 + e^{-\lambda\tau_2}\left(c_1\lambda^2 + c_2\lambda + c_3\right) = 0. \tag{44}$$

For the stability changes to occur, we have to show that there exists a pair of purely imaginary roots of the characteristic equation for a critical value of $\tau_2 > 0$. Suppose that there exists a purely imaginary root say $i\Xi$ of equation (44).

We substitute $\lambda = i\Xi$ in (44) and then, separating the real and imaginary parts, we finally obtain

$$\begin{aligned} \Xi^4 - a_2\Xi^2 + a_4 &= \left[\Xi^2 c_1 - c_3\right]\cos\Xi\tau_2 - [\Xi c_2]\sin\Xi\tau_2, \\ a_1\Xi^3 - a_3\Xi &= \left[\Xi^2 c_1 - c_3\right]\sin\Xi\tau_2 + [\Xi c_2]\cos\Xi\tau_2. \end{aligned} \tag{45}$$

By squaring and adding the above two equations

$$\Xi^8 + \alpha_1\Xi^6 + \alpha_2\Xi^4 + \alpha_3\Xi^2 + \alpha_4 = 0. \tag{46}$$

Substituting $\Xi^2 = \ell$ in equation (46), we get the following equation:

$$\ell^4 + \lambda_1\ell^3 + \lambda_2\ell^2 + \lambda_3\ell + \lambda_4 = 0, \tag{47}$$

where

$$\lambda_1 = a_1^2 - 2a_2, \quad \lambda_2 = 2a_4 + a_2^2 - 2a_1a_3 - B_1^2,$$
$$\lambda_3 = -2a_4a_2 + a_3^2 + 2c_1c_3 - c_2^2, \quad \lambda_4 = a_4^2 - c_3^2.$$

Let us define $H(l)$ by

$$H(l) = \ell^4 + \lambda_1\ell^3 + \lambda_2\ell^2 + \lambda_3\ell + \lambda_4. \tag{48}$$

All roots of equation (48) have negative real parts if and only if the Routh – Hurwitz conditions given in (49) hold. Consequently, the endemic equilibrium E^* is locally asymptotically stable for any $\tau_2 > 0$, provided that the following conditions are satisfied:

$$\lambda_1 >, \quad \lambda_4 > 0, \quad \lambda_1\lambda_2 - \lambda_3 > 0, \quad (\lambda_1\lambda_2 - \lambda_3)\lambda_3 - \lambda_1^2\lambda_4 > 0. \tag{49}$$

If $\lambda_4 < 0$ Eq. (48) possesses at least one positive root $m > 0$. Then we find $\pm i\sqrt{m}$ to be a root of (46) corresponding to the delay τ_2^*. The endemic equilibrium E^* remains stable for $\tau_2 < \tau_2^*$, the latter being a critical value of the delay under which the delayed system (5) remains stable. To determine it, from Eq. (45) we have

$$\tau_2^* = \frac{1}{m}\cos^{-1}\left[\frac{m^2c_3\left[a_1m^2 - a_3\right] + \left(c_1m^2 - B_3\right)\left[m^4 - a_2m^2 + D_4\right]}{\left(c_1m^2 - B_3\right)^2 + c_2^2m^2}\right] + \frac{2\pi n}{m}, \quad n = 0,\ 1,\ 2,\ 3,\ \ldots \tag{50}$$

Thus, in summary we have the following result.

If $\lambda_4 < 0$ is satisfied the steady-state E^* is locally asymptotically stable for $\tau_2 < \tau_2^*$ and becomes unstable for $\tau_2 > \tau_2^*$. Furthermore, the system will undergo a Hopf bifurcation at E^* when $\tau_2 = \tau_2^*$ provided that

$$4m^6 + \pi_1m^4 + \pi_2m^2 + \pi_3 > 0, \tag{51}$$

with $\pi_1 = 3a_1 - 6a_2$, $\pi_2 = 2a_2 + 4a_4 - 4a_1a_3 - 2c_1^2$, $\pi_3 = a_3^2 - 2a_2a_4 - c_2^2 + 2c_1c_3$. Differentiating (45) with respect to τ_2, we get

$$\frac{d\tau_2}{d\xi} = \frac{4\xi^3 + 3\left(a_1\xi^2 + 2a_2\xi + a_3\right)}{c_1\xi^3 + c_2\xi^2 + B_3\xi}e^{\xi\tau_2} + \frac{2c_1\xi + c_2}{c_1\xi^3 + c_2\xi^2 + B_3\xi} - \frac{\tau_2}{\xi}. \tag{52}$$

Hence,

$$\operatorname{sgn}\left[\frac{d}{d\tau_2}\operatorname{Re}(\xi)\right]_{\tau_2=\tau_2^*} = \operatorname{sgn}\left[\operatorname{Re}\left(\frac{d\xi}{d\tau_2}\right)^{-1}\right]_{\xi=im} = \operatorname{sgn}\left[\frac{4m^6 + \pi_1m^4 + \pi_2m^2 + \pi_3}{c_2m^2 + \left[-c_1m^2 + B_3\right]^2}\right]. \tag{53}$$

Now $\operatorname{sgn}\left[\frac{d}{d\tau_2}\operatorname{Re}(\xi)\right]_{\tau_2=\tau_2^*} > 0$ if the numerator is positive, i. e., the transversality condition holds (51) and the system undergoes a Hopf bifurcation at $\tau_2 = \tau_2^*$.

Case IV: When $\tau_1 = \tau_2 = \tau > 0$

Equation (29) becomes

$$\lambda^4 + a_1\lambda^3 + a_2\lambda^2 + a_3\lambda + a_4 + e^{-\lambda\tau}\left(l_1\lambda^3 + l_2\lambda^2 + l_3\lambda + l_4\right) = 0, \tag{54}$$

where $l_1 = b_1$, $l_2 = b_2 + c_1$, $l_3 = b_3 + c_2$, $l_4 = b_4 + c_3$.

This analysis is similar to that for case II.

4. Sensitivity analysis

The effect of different parameter values on the functional value of the basic reproduction number R_0 is investigated in this section. Identifying the most influential parameters is crucial, as they provide effective criteria for pest management strategies. Each parameter of the model significantly affects the pest dynamics. Hence, a sensitivity analysis of the basic reproduction number with respect to all model parameters is performed.

The basic reproduction number is given by

$$R_0 = \frac{\alpha\eta e^{-d_1\tau_1}}{\gamma r + \eta d_2}. \tag{55}$$

The partial derivatives of R_0 with respect to the parameters η, α, γ, d_1, d_2, and r are computed as follows:

$$\begin{aligned} &\frac{\partial R_0}{\partial \eta} = \frac{\alpha e^{-d_1\tau_1}(\gamma r)}{(\gamma r + \eta d_2)^2}, \quad \frac{\partial R_0}{\partial \alpha} = \frac{\eta e^{-d_1\tau_1}}{\gamma r + \eta d_2}, \quad \frac{\partial R_0}{\partial \gamma} = -\frac{\alpha\eta r e^{-d_1\tau_1}}{(\gamma r + \eta d_2)^2}, \\ &\frac{\partial R_0}{\partial d_1} = -\tau_1 R_0, \quad \frac{\partial R_0}{\partial d_2} = -\frac{\alpha\eta^2 e^{-d_1\tau_1}}{(\gamma r + \eta d_2)^2}, \quad \frac{\partial R_0}{\partial r} = -\frac{\alpha\eta\gamma e^{-d_1\tau_1}}{(\gamma r + \eta d_2)^2}. \end{aligned} \tag{56}$$

The normalized forward sensitivity (elasticity) index is defined as

$$E_p = \frac{p}{R_0}\frac{\partial R_0}{\partial p}, \tag{57}$$

where p denotes any parameter.

Accordingly, the sensitivity indices of R_0 are given by

$$\begin{aligned} E_\eta &= \frac{\gamma r}{\gamma r + \eta d_2} > 0, \\ E_\alpha &= 1, \\ E_\gamma &= -\frac{\gamma r}{\gamma r + \eta d_2} < 0, \\ E_{d_1} &= -\tau_1 d_1 < 0, \\ E_{d_2} &= -\frac{\eta d_2}{\gamma r + \eta d_2} < 0, \\ E_r &= -\frac{\gamma r}{\gamma r + \eta d_2} < 0. \end{aligned} \tag{58}$$

It is observed that the sensitivity indices E_α and E_η are positive, indicating that an increase in the pest reproduction rate α or the awareness decay rate η leads to an increase in the basic reproduction number R_0. In contrast, the parameters γ, d_1, d_2, and r exhibit negative sensitivity indices, implying that increasing awareness effectiveness, pest mortality, or awareness dissemination reduces the invasion potential of the pest population.

These results demonstrate that R_0 is most sensitive to changes in the pest reproduction rate and the maturation delay parameters. Even small perturbations in highly sensitive parameters can lead to significant changes in pest dynamics. Therefore, careful estimation and control of these parameters are essential for effective pest management, as illustrated in Fig. 1.

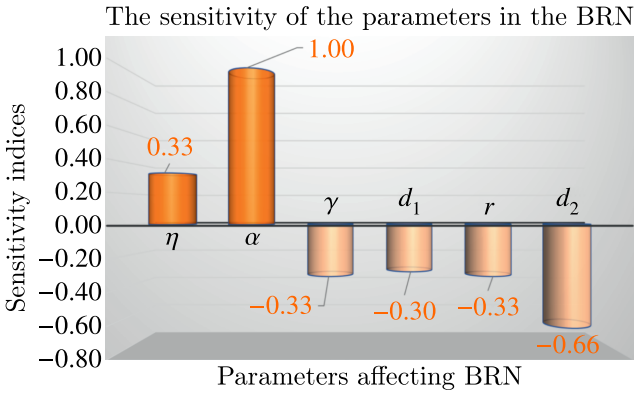

Figure 1. Sensitivity analysis: plot of sensitivity indices of different parameters affecting the reproduction number R_0

5. Numerical examples

A few representative numerical simulations are presented in this section. The parameter values used in the simulations are chosen from biologically realistic ranges reported in the literature on rugose spiraling whitefly, parasitoid dynamics, and awareness-based pest management [Al Basir et al., 2019; Abraha et al., 2021; Suganya et al., 2024]. These choices are consistent with field observations from major coconut-growing regions of Tamil Nadu, particularly Pollachi, which has experienced severe rugose spiraling whitefly infestation [Selvaraj et al., 2017; Rao et al., 2018]. Thus, the simulations reflect biologically realistic regimes reported in plantation studies. The egg-laying rate α and the maturation delay τ_1 are selected based on documented life-cycle characteristics and fecundity of rugose spiraling whitefly under tropical climatic conditions [Elango, Nelson, 2020; Saranya et al., 2021]. The natural mortality rates d_1 and d_2 represent environmental and biological mortality observed in field populations. The parasitization rate ϕ and the conversion efficiency ϕ_1 reflect the effectiveness of the parasitoid *Encarsia guadeloupae* in suppressing immature rugose spiraling whitefly stages, as reported in field studies from Tamil Nadu, including Pollachi [Selvaraj et al., 2020; Suriya et al., 2021]. The initial conditions used in the numerical simulations are assumed as $(X(0), Y(0), S(0), A(0)) = (0.2, 0.15, 0.1, 0.1)$ to represent an early-stage infestation with low but nonzero pest density, parasitoid presence, and farmer awareness. These values ensure biological feasibility of the model and allow the long-term effects of maturation and awareness delays on system dynamics to be examined without loss of generality.

From Fig. 2, we see that an increase in the egg laying rate α intensifies pest reproduction, resulting in higher immature and mature pest densities and a corresponding increase in awareness, whereas the parasitoid population shows limited growth. Figure 3 demonstrates that an increase in the maturation delay τ_1 leads to a slower decline of the immature pest population and a significant decrease in the mature pest density. This delay in pest maturation indirectly reduces parasitoid abundance due to limited host availability, whereas the awareness level exhibits a delayed but increasing trend with larger τ_1. Figure 4 highlights the influence of the awareness response delay τ_2 on the system dynamics. It is observed that increasing τ_2 weakens the effectiveness of awareness-based control, leading to higher mature pest densities and a slower decline of the immature pest population. These results emphasize the importance of timely awareness dissemination in effective pest management. Figure 5, *a*, illustrates the dynamical behavior of system (5) for the parameter set $\alpha = 0.01$, $\phi = 0.001$, $d_1 = 0.01$, $d_2 = 0.02$, $d_3 = 0.02$, $\phi_1 = 0.6$, $r_0 = 0.003$, $h = 0.012$, $\eta = 0.015$, and $\gamma = 0.005$, with fixed delays $\tau_1 = 30$ and $\tau_2 = 10$. For these values, the basic reproduction number satisfies $R_0 < 1$, implying that the pest-free equilibrium is stable. For $\alpha = 0.05$ with the other values being the same, from Fig. 5, *b*, the numerical

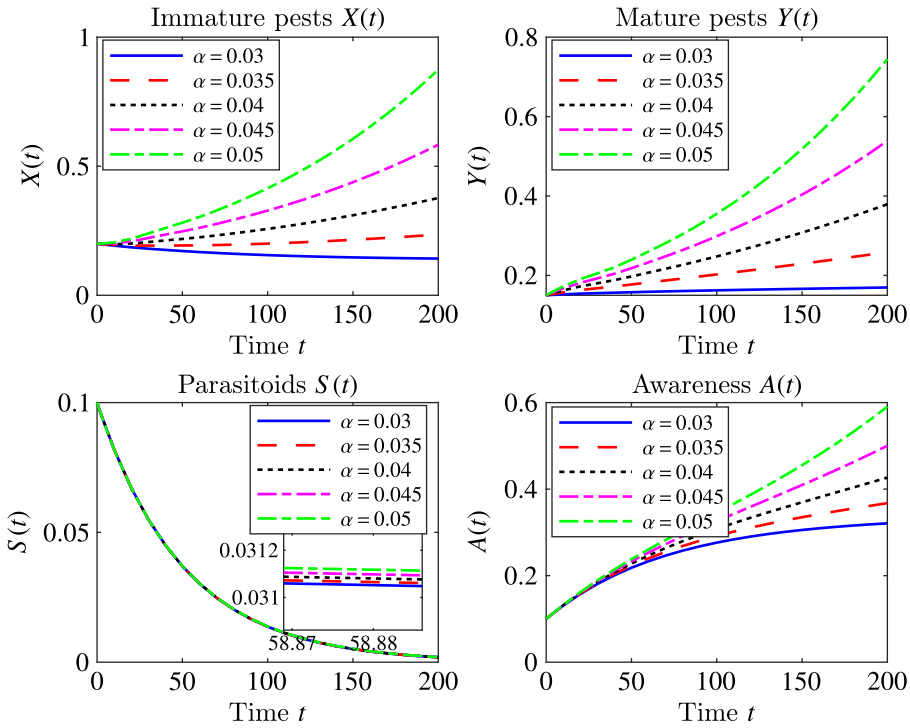

Figure 2. Time series of immature pests $X(t)$, mature pests $Y(t)$, parasitoids $S(t)$, and awareness level $A(t)$ for different values of the egg laying rate α

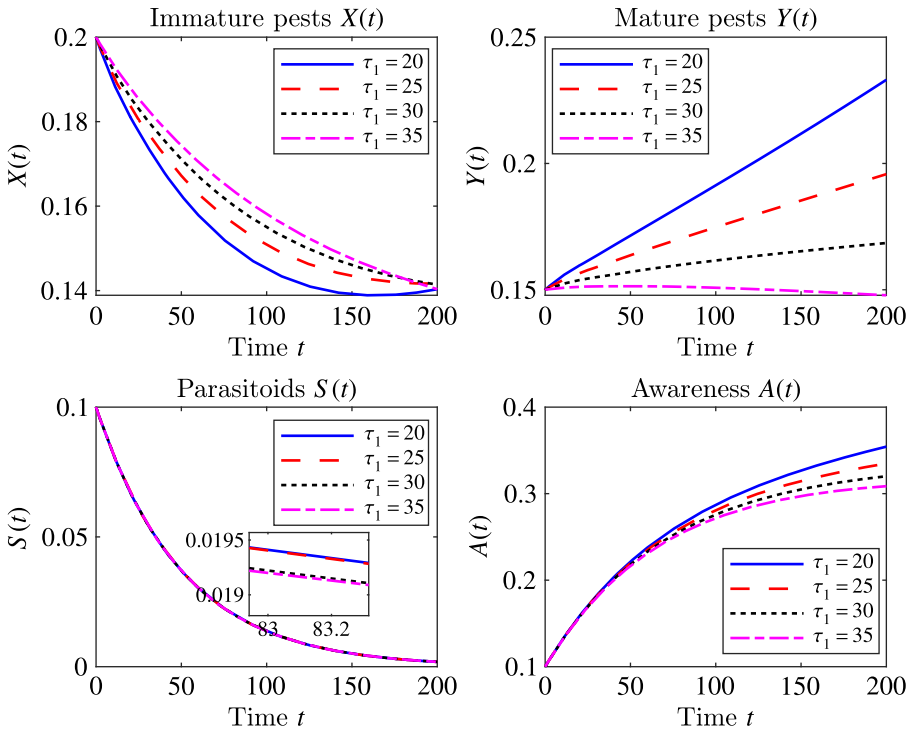

Figure 3. Time series of immature pests $X(t)$, mature pests $Y(t)$, parasitoids $S(t)$, and awareness level $A(t)$ for different values of the egg laying rate τ_1

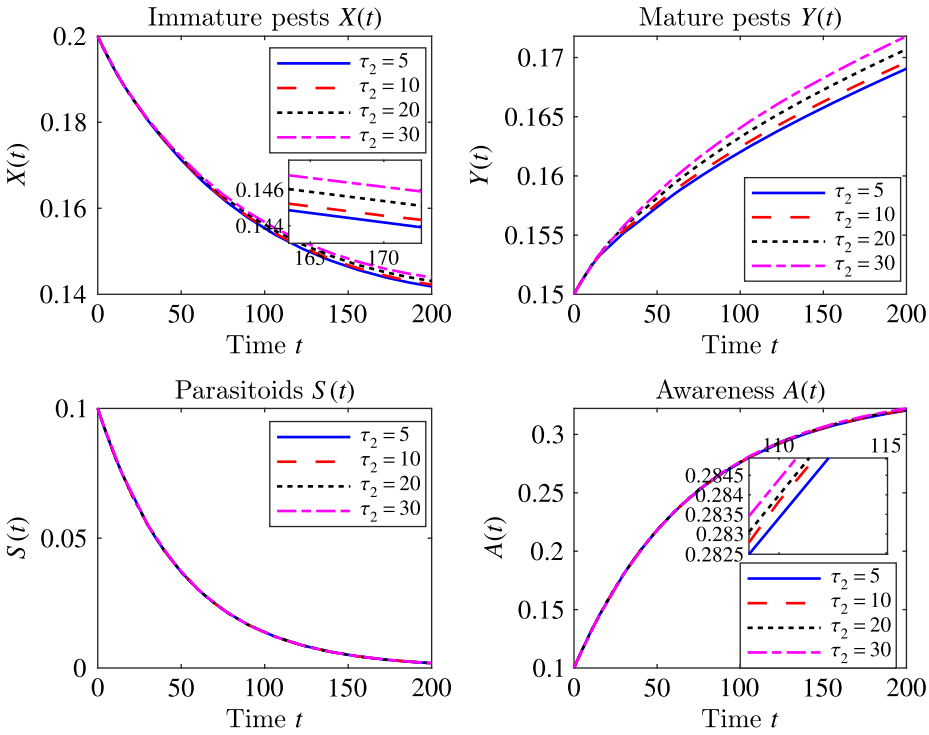

Figure 4. Time series of immature pests $X(t)$, mature pests $Y(t)$, parasitoids $S(t)$, and awareness level $A(t)$ for different values of the egg laying rate τ_2

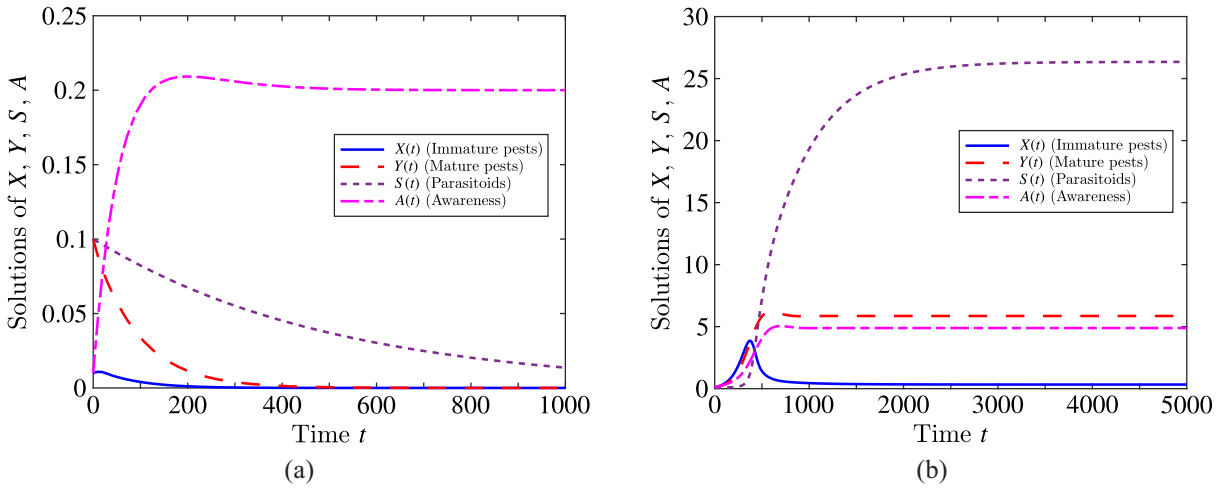

Figure 5. Dynamics of system variables illustrating (a) pest-free equilibrium for $\alpha = 0.01$ ($R_0 < 1$) and (b) endemic equilibrium for $\alpha = 0.05$ ($R_0 > 1$)

simulations show that all state variables converge to a positive equilibrium, indicating the existence of a coexistence equilibrium where immature pests, mature pests, parasitoids, and the awareness level coexist. This numerical observation confirms the analytical result that, when $R_0 > 1$, the pest-free equilibrium becomes unstable and the system admits a biologically meaningful coexistence state. From Figs. 6, *a* and 6, *b*, it is observed that increasing either the awareness-induced mortality rate γ or the baseline awareness program rate r significantly reduces the mature pest population $Y(t)$, demonstrating the crucial role of awareness-based interventions in pest suppression. From Figs. 7, *a* and 7, *b*, an increase in the parasitization rate ϕ accelerates the reduction of immature pests, whereas a higher

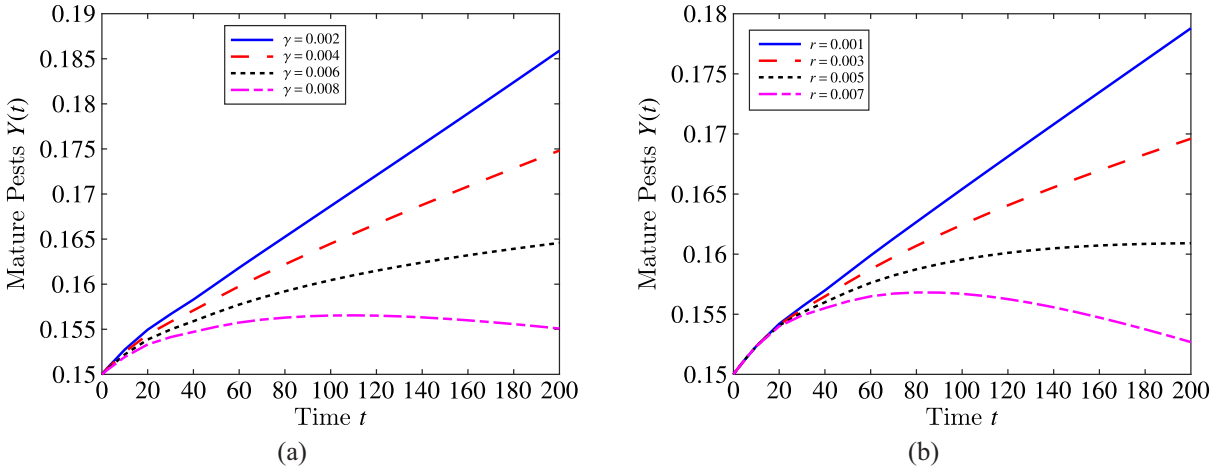

Figure 6. Effect of awareness-related parameters on the mature pest population $Y(t)$: (a) effect of the awareness-induced mortality rate γ, (b) effect of the baseline rate of awareness programs r

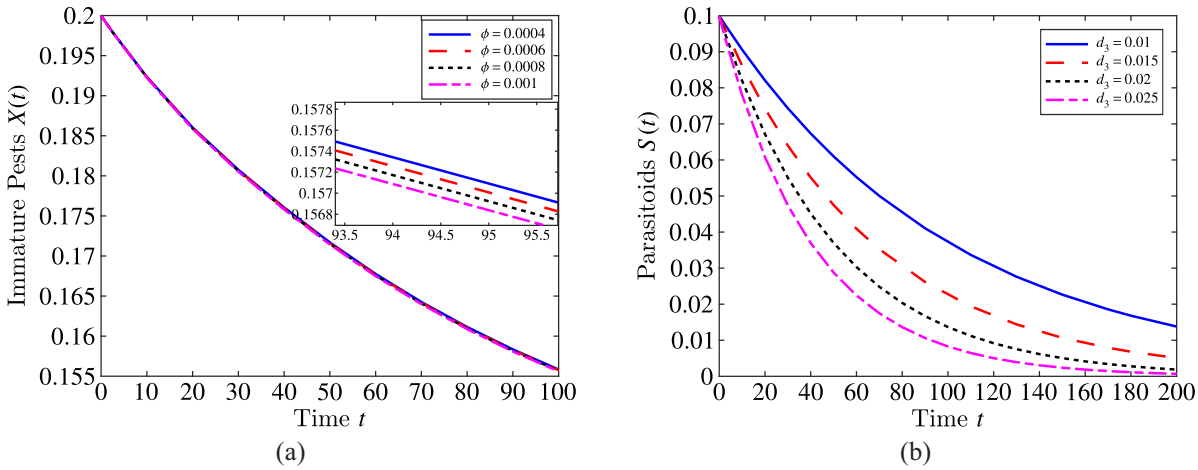

Figure 7. Effect of biological control parameters: (a) effect of the parasitization rate ϕ on the immature pest population $X(t)$, (b) effect of the parasitoid mortality rate d_3 on the parasitoid population $S(t)$

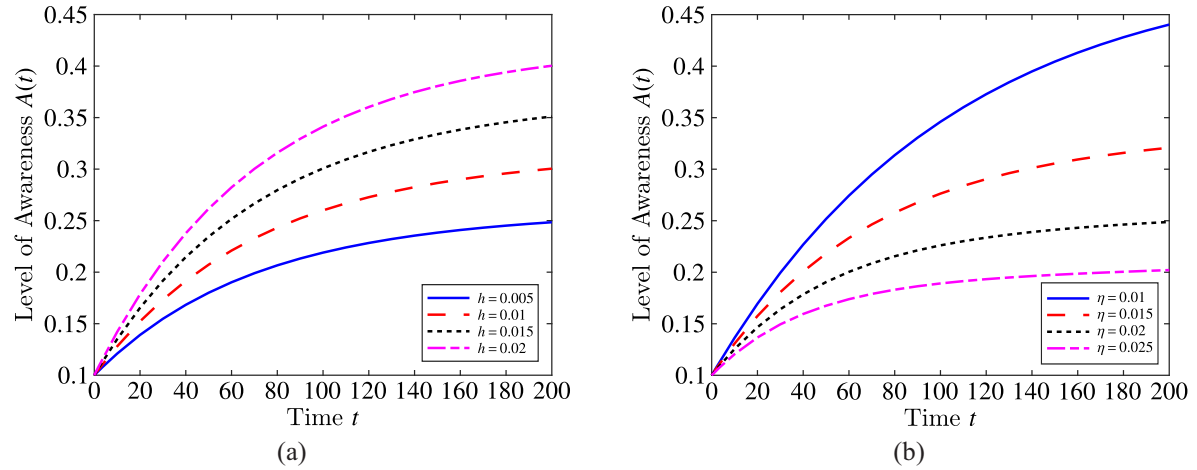

Figure 8. Effect of awareness parameters on the awareness level $A(t)$: (a) effect of the local awareness gain rate h, (b) effect of the awareness fading rate η

parasitoid mortality rate d_3 leads to a rapid decline in the parasitoid population. From Figs. 8, *a* and 8, *b*, an increase in the awareness gain rate h enhances the buildup of awareness, whereas a higher fading rate η diminishes the long-term awareness level. For the parameter values considered, the numerical solutions approach steady states without sustained oscillations, reflecting the stabilizing influence of parasitoid pressure and awareness-based control through strong negative feedback. Such dynamics are consistent with regulated pest management scenarios. Overall, the results demonstrate the effectiveness of awareness dissemination and biological control in curbing pest populations.

Table 1. Parameter descriptions and values used for analysis [Al Basir et al., 2019; Abraha et al., 2021; Suganya et al., 2024]

Symbol	Description	Unit	Value/Range used
α	Egg laying rate of mature pests	$\text{pest}^{-1}\ \text{day}^{-1}$	0.01–0.05
ϕ	Parasitization rate of immature pests	$\text{parasite}^{-1}\ \text{day}^{-1}$	0.0004–0.001
d_1	Natural mortality rate of immature pests	day^{-1}	0.005–0.02
d_2	Natural mortality rate of mature pests	day^{-1}	0.02–0.04
ϕ_1	Conversion efficiency of parasitoids	dimensionless	0.2–0.6
d_3	Natural mortality rate of parasitoids	day^{-1}	0.002–0.03
γ	Awareness-induced mortality rate of mature pests	day^{-1}	0.002–0.008
r	Baseline rate of awareness programs	day^{-1}	0.001–0.007
h	Rate of local awareness increase due to pests	day^{-1}	0.005–0.02
η	Fading rate of awareness	day^{-1}	0.01–0.025
τ_1	Maturation delay of immature pests	days	20–40
τ_2	Awareness response delay	days	5–30

6. Conclusion

This study has developed a stage-structured mathematical model incorporating key biological and behavioral delays, namely, maturation delay and delay in awareness spread, to investigate the control of rugose spiraling whitefly in coconut plantations. By combining parasitoid-based biological control with awareness-driven interventions, the model provides a realistic and practical framework for pest management. The present study offers a qualitative theoretical perspective on how maturation and awareness delays influence rugose spiraling whitefly dynamics. Analytical results and numerical simulations show that timely biological control and awareness-based interventions can lead to effective pest suppression, while delays may affect the rate at which the system approaches equilibrium. The stability analysis identifies threshold conditions for successful control and highlights how delays can either enhance or hinder control effectiveness depending on their timing. Overall, this work offers qualitative theoretical insight into stability and control thresholds in stage-structured pest dynamics.

Conflict of interest

The authors declare that there is no conflict of interest.

Acknowledgements

We sincerely thank the reviewers for their valuable comments, which were of great help in revising the manuscript. It is our pleasure to thank the College of Engineering and Technology, SRM Institute of Science and Technology for its valuable support and constant encouragement.

References

Abraha T., Al Basir F., Obsu L. L., Torres D. F. Pest control using farming awareness: Impact of time delays and optimal use of biopesticides // Chaos, Solitons & Fractals. — 2021. — Vol. 146. — Article 110869.

Aiello W. G., Freedman H. I. A time-delay model of single-species growth with stage structure // Mathematical Biosciences. — 1990. — Vol. 101, No. 2. — P. 139–153.

Al Basir F. A multi-delay model for pest control with awareness-induced interventions // International Journal of Biomathematics. — 2020. — Vol. 13, No. 6. — P. 2050047.

Al Basir F., Elaiw A. M., Ray S. Effect of time delay in controlling crop pest using farming awareness // International Journal of Applied and Computational Mathematics. — 2019. — Vol. 5. — P. 1–19.

Al Basir F., Ray S., Venturino E. Role of media coverage and delay in controlling infectious diseases // Applied Mathematics and Computation. — 2018. — Vol. 337. — P. 372–385.

An Q., Beretta E., Kuang Y., Wang C., Wang H. Geometric stability switch criteria in delay differential equations // Journal of Differential Equations. — 2019. — Vol. 266, No. 11. — P. 7073–7100.

Bandyopadhyay M., Banerjee S. A stage-structured prey – predator model with discrete time delay // Applied Mathematics and Computation. — 2006. — Vol. 182, No. 2. — P. 1385–1398.

Banerjee S., Mukhopadhyay B., Bhattacharyya R. Effect of maturation and gestation delays in a stage-structured predator – prey model // Journal of Applied Mathematics & Informatics. — 2010. — Vol. 28, No. 5–6. — P. 1379–1393.

DeBach P., Rosen D. Biological control by natural enemies. — Cambridge: Cambridge University Press, 1991.

Dhaliwal G. S., Arora R. Principles of insect pest management. — New Delhi: Kalyani Publishers, 1996.

Dhivyadharshini B., Senthamarai R. Modeling rugose spiraling whitefly infestation using delay differential equations // European Journal of Pure and Applied Mathematics. — 2024. — Vol. 17, No. 3. — P. 1908–1936.

Elango K., Nelson S. J. Effect of host plants on the behaviour of rugose spiraling whitefly and their natural enemies // Research Journal of Agricultural Sciences. — 2020. — Vol. 11, No. 1. — P. 120–123.

Govindaraj S., Rathinam S. Mathematical modeling of the effect of rugose spiraling whitefly on coconut trees // AIMS Mathematics. — 2022. — Vol. 7, No. 7. — P. 13053–13073.

Hale J. K. Functional differential equations. — New York: Springer, 1969.

Heffernan J. M., Smith R. J., Wahl L. M. Perspectives on the basic reproductive ratio // Journal of the Royal Society Interface. — 2005. — Vol. 2, No. 4. — P. 281–293.

Huang Y. Delay differential equations with applications to population dynamics. — New York: Academic Press, 1993.

Ismail H., Debbouche A., Hariharan S., Shangerganesh L., Kashtanova S. V. Stability and optimality criteria for an SVIR epidemic model // Mathematics. — 2024. — Vol. 12, No. 20. — Article 3231.

Jatav K. S., Dhar J., Nagar A. K. Mathematical study of stage-structured pests control through impulsively released natural enemies with discrete and distributed delays // Applied Mathematics and Computation. — 2014. — Vol. 238. — P. 511–526.

Khan G. A., Muhammad S., Mahmood Ch. K., Khan M. A. Information regarding agronomic practices and plant protection measures obtained by farmers through electronic media // Journal of Agricultural Research. — 2013. — Vol. 51. — P. 123–130.

Kumar V., Dhar J., Bhatti H. S. A stage-structured pest–natural enemy dynamics with Holling type-II interaction and maturation delay // Environmental Modeling & Assessment. — 2019. — Vol. 24. — P. 355–363.

Mathur K. S., Srivastava A., Dhar J. Dynamics of a stage-structured SI model with media-induced response // Journal of Engineering Mathematics. — 2021. — Vol. 127. — P. 1–21.

Rao N. C., Roshan D. R., Rao G. K., Ramanandam G. A review on rugose spiraling whitefly in India // Journal of Pharmacognosy and Phytochemistry. — 2018. — Vol. 7, No. 5. — P. 948–953.

Santra N., Sahoo D., Mondal S., Samanta G. An epidemiological multi-delay model on cassava mosaic disease // Filomat. — 2023. — Vol. 37, No. 6. — P. 2887–2921.

Saranya M., Kennedy J. S., Jeyarani S., Anandham R., Bharathi N. Life cycle and morphometry of rugose spiraling whitefly, *Aleurodicus rugioperculatus* Martin (Hemiptera: Aleyrodidae) on coconut // Journal of Applied and Natural Science. — 2021. — Vol. 13 (SI). — P. 100.

Selvaraj K., Gupta A., Venkatesan T., Jalali S. K., Sundararaj R., Ballal C. R. First record of invasive rugose spiraling whitefly along with parasitoids in Karnataka // Journal of Biological Control. — 2017. — P. 74–78.

Selvaraj K., Sumalatha B. V., Poornesha B., Ramanujam B., Shylesha A. N. Biological control of invasive rugose spiraling whitefly in coconut // Journal of Biological Control. — 2020.

Singh H., Dhar J., Bhatti H. S., Chandok S. An epidemic model of childhood disease dynamics with maturation delay // Modeling Earth Systems and Environment. — 2016. — Vol. 2. — P. 1–8.

Suganya G., Jenitta E., Senthamarai R. A study on the dynamics of pest population with biocontrol using predator and parasite in the presence of awareness // Computer Research and Modelling. — 2024. — Vol. 16, No. 3. — P. 713–729.

Suganya G., Senthamarai R. Analytical approximation of a nonlinear model for pest control in coconut trees // Computer Research and Modelling. — 2022a. — Vol. 14, No. 5. — P. 1093–1106.

Suganya G., Senthamarai R. Impact of awareness on the dynamics of pest control in coconut trees // Engineering Letters. — 2022b. — Vol. 30, No. 4.

Suriya S., Preetha G., Balakrishnan N., Sheela J. Natural parasitization of *Encarsia guadeloupae* on coconut rugose spiraling whitefly // The Pharma Innovation Journal. — 2021. — Vol. 10. — P. 388–390.

Yang X., Chen L., Chen J. Permanence and positive periodic solutions of nonautonomous delay models // Computers & Mathematics with Applications. — 1996. — Vol. 32, No. 4. — P. 109–116.

Zhou W., Arcot Y., Medina R. F., Bernal J., Cisneros-Zevallos L., Akbulut M. E. Integrated pest management: sustainability approach to crop protection // ACS Omega. — 2024. — Vol. 9, No. 40. — P. 41130–41147.